JOURNAL OF ENGINEERING SCIENCES

Volume 7, Issue 2 (2020)

Olakunle M.S., Ameh A.O., Oyegoke T., Shehu H.U. (2020). Effect of ethyl acetate, time and particle size on the kinetics of the oleoresin extraction process. Journal of Engineering Sciences, Vol. 7(2), pp. F15–F23, doi: 10.21272/jes.2020.7(2).f3.

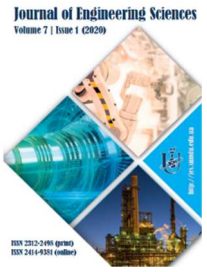

Effect of Ethyl Acetate, Time and Particle Size on the Kinetics of the Oleoresin Extraction Process

Olakunle M.S.[1], Ameh A.O.[1], Oyegoke T.[1, 3*[0000-0002-2026-6864]], Shehu H.U.[2]

[1] Chemical Engineering Department, Ahmadu Bello University Zaria, Nigeria;
[2] Chemical Engineering Technology Department, Kaduna Polytechnic, Kaduna, Nigeria;
[3] Laboratoire de Chimie, ENS l'Universite de Lyon, 69007, France

Article info:
Paper received: June 30, 2020
The final version of the paper received: October 10, 2020
Paper accepted online: October 21, 2020

***Corresponding email:**
OyegokeToyese@gmail.com

Abstract. The kinetics of the extraction of oleoresin from ginger using ethyl acetate as the solvent was studied in this work. The effects of particle size and extraction time on oleoresin's solvent extraction were analyzed to obtain optimization data. The temperature of the process was kept constant at 40 °C. The Ginger particle sizes ranged between 250–1200 μm at extraction times ranging between 10–70 min. Experimental data generated were fitted into an empirical model to determine the kinetic parameters. The oleoresin yield increases with increasing extraction time up to an optimum time, after which the yield remains constant and decreasing particle size. The results obtained for the kinetics studies reveal that with the introduction of the constant term accounting for the diffusion step separately (as an addition) into a single step first-order model (Patricelli's first order model) raises from 87 % fitness of the model into becoming 99 % with the experimental data. And this improved form of Patricelli's first-order model was found to have shown as good agreement with Patricelli's 2-step kinetic model. These findings further confirm the oleoresin extraction process in the presence of ethyl acetate was found to be first-order kinetics involving two steps mechanism where the use of a single-step first-order model (Patricelli's first-order kinetic model) and the choice of using ethyl acetate must have contributed to the strong resistance present in the first step of the extraction mechanism especially for the smaller particle size (250 μm). In getting the extraction yield improved, this study, therefore, recommends the use of small particle sizes (< 250 μm), higher temperatures (> 40 °C), and better alternative solvents like ethanol.

Keywords: ethyl acetate, extraction, oleoresin, modeling.

1 Introduction

Oleoresins are the flavor extracts obtained from ground spices. They have an aroma of spice and possess the attributes which contribute to the taste. Ginger species exhibit aromatic properties of commercial importance

One is an essential oil, which varies between 0.8–4.2 %, while the other is oleoresin in the range of about 7 % depending on its habitat, origin, and agronomic treatment of culture (Azian et al., 2001). The pungent taste of ginger is due to non-volatile phenylpropanoid derived compounds, particularly gingerols and shogaols. Oleoresin from ginger's rhizomes mainly comprises essential oil, 6-gingerol, the principal pharmacologically active component, and a lesser amount of a structurally related vanilloid (Bode and Dong, 2004).

The increased prominence of oleoresins over natural spices is due to the advantages that oleoresins have over the spices themselves. These advantages include more uniform flavor and concentration and a lack of microbial contamination. The ginger oleoresin is widely used as a flavoring agent in food, drink, and medicine.

Oleoresin compounds, such as 6-gingerol and its derivatives, are sourced from a ginger root with high et al., 2007). The antioxidants are trace nutrients that have become a subject of interest in recent years due to their ability to neutralize free radicals' effects. (Carenas and Packer, 1996). Furthermore, the report of Mbaeyi-Nwaoha et al. (2013) and Sies (1996) indicated that these free radicals are potentially harmful products released during a series of natural processes taking place in a living body and are associated with the aging of cells and tissues. If you do not suppress the active oxygenates, the long term can lead to cardiovascular disease, diabetes, cancer, arthritis, and other neurodegenerative disorders.

The significance of these polyphenolic compounds cannot be overemphasized. It possesses several vital properties like digestion boosting effect by exerting a stimulating effect on peptic juices, such as gastric juice, bile, pancreatic and intestinal juices (Platel and Srinivasan, 1996). A survey of literature also indicated that the 6-gingerol possesses anti-bacterial, anti-inflammatory, anti-tumor-promoting, and anti-angiogenic activities (Kim et al., 2005). Studies have shown that scientific interest and some popularity in testing essential oils and plant extracts to identify the characteristics of natural compounds and antioxidant activity and antimicrobial activity that are used medically worldwide. (Hassan et al., 2012).

Solvent extraction and steam distillation are established conventional methods for extracting oleoresin from ginger (Akhihiero et al., 2013). Solvent extraction is a widely used technique designed to separate soluble polyphenols from plant tissue using a solvent. Often used solvents to extract oleoresin from plant tissue - water, ethanol, methanol, acetone, and many others. (Jakopic et al., 2009; Salmon et al., 2012). Extraction methods to obtain bioactive compounds from ginger include heat-reflux extraction (HRE). Kim et al. (2014) stated that HRE is a conventionally solvent-extraction method widely used in herbal medicine preparation. It is close to the traditional extraction method of an herbal formula. In the HRE process, the solvent is boiled, and the vapor generated is allowed to condense to droplets in the attached condenser on the flask; hence, the temperature and pressure are not variables to be chosen as extraction parameters.

Other novel extraction methods include microwave-assisted extraction (MAE), supercritical fluid extraction, and pressurized solvent extraction has drawn significant research attention in the last two decades (Zhiyi et al., 2006; Ismail et al., 2013). In MAE, the increase in the extract recovery by microwave is generally attributed to its volumetric heating effect, which occurs due to the solvent's dipole rotation in the microwave field. This heating effect causes the solvent temperature to rise, increasing the solubility of the compounds of interest. In particular, solvent heating by microwave occurs when molecules of the polar solvent cannot align themselves quickly enough to the high-frequency electric field (typically 2450 MHz) of a microwave, thereby causing the solvent molecules to dissipate the absorbed energy in the form of heat (Hemwimon et al., 2007).

Although many studies have been carried out on the determination of the active compounds of ginger and the development and implementation of the different operating conditions for ginger oleoresin recovery (Bartley and Jacobs, 2000). Little attention seems to have been given to the optimization of the various extraction variables (e.g., the appropriate solvent, temperature, contact time, quantity of sample, and many others) or a systematic study for optimizing the method been carried out. However, Mukherjee et al. (2014) were able to carry out an optimization study for the process via three influential parameters like ethanol concentration, temperature, and extraction time. Likewise, Ok and Jeong (2012) determined the optimum conditions for obtaining a 6-Shogaol-rich extract from ginger via the use of some selected factors to determine the optimum yield and high antioxidant properties. While Kanadea and Bhatkhandeb (2016) also reported the efficacy of solvent extraction for obtaining ginger oil. Other works that study the extraction of oleoresin is Saidi et al. (2014) employed the use of ultrasonic sound-assisted, while Nguyen et al. (2018) determined the optimum condition via the use of microwave-assisted energy in their process. In recent times, Ameh et al. (2020) evaluated the influence of change in extraction time and particle size on the rate of oleoresin extraction from ginger rhizomes.

However, this present study aimed to provide insight into ethyl acetate's significance in oleoresin extraction from the ginger rhizome. The study also investigated the influence of particle size and extraction time on the yield of oleoresin. Furthermore, extraction kinetics prediction models for the yield of oleoresin were developed via the curve fitting approach, which aided with using tools like MATLAB and Python algorithm. The study's focus was mainly on Nigeria's ginger variety, which was reported to be available in abundance.

2 Research Methodology

2.1 Ginger procurement, pretreatment, and preliminary analysis

Ginger rhizomes were sourced from Jaba local government in the southern part of Kaduna state, North-Central Region of Nigeria. Proximate and FTIR analysis of the ginger samples were collected from our previous studies (Alewo et al., 2020). The samples were washed thoroughly with water to remove sand and dirt. The light outer skin was scraped off and cut into tiny pieces. All samples so prepared were dried in an air-circulating oven at a temperature of 40^{o}C in the laboratory and ground manually into power and sieved into five different particle sizes of 1200, 850, 600, 425, and 250 microns. The samples were stored in air-tight polythene bags as stock samples in a cool, dry place until required for extraction.

2.2 Oleoresin extraction

Ten grams of 1200 μm powdered ginger was placed directly into a round bottom flask containing 100ml of the solvent (95 % ethyl acetate); the round bottom flask was placed in a hot water bath which sat on a combined hot plate and stirrer. Both the water bath and solvent mixture was stirred throughout the extraction time of 10 min. The round bottom flask has three ports. The water-cooled condenser was connected directly to the round bottom flask using one of the ports. The temperature was kept constant at 40 ± 2 °C, and the system was operated at atmospheric pressure. After the solvent was extracted, the distillation method using a soxhlet extractor to obtain a solvent-free oleoresin. The recovered oleoresin was then cooled and weighed.

Five different particle sizes of 1200, 850, 600, 425, and 250 microns of the powdered ginger samples were used to study the effect of particle size at a constant temperature of 40^{o}C, a solid-liquid ratio of 10g/100ml solvent while

varying the extraction time between 10 and 70 minutes at an interval of 10 minutes. After each run, the solvent was separated from the oleoresin by distillation to obtain solvent-free oleoresin.

2.3 Determination of the yield

The oleoresin yield was calculated using the following formula:

$$Y\ (\%) = \frac{Wo}{Wd} \times 100, \quad (1)$$

where Y – oleoresin yield, %; Wo – the weight of oleoresin extracted, g; Wd – the used weight of dried ginger powder, g.

The extracted oleoresin was characterized using FTIR (FTIR ABB3000) at the Center for Mineral Research and Development, Kaduna Polytechnic, Kaduna, Nigeria.

2.4 Extraction kinetic studies and modeling

A first-order model (Ana-marija et al., 2018; Kasuma and Mahfud, 2017) is proposed to describe the kinetics of ginger rhizome's oleoresin extraction. The model assumes a mass transfer/diffusion mechanism. The mass transfer of oleoresin during solvent extraction can be described by a first-order model (Ozkal et al., 2005). The kinetics model equation is:

$$\tau \frac{dY}{dt} = (K - Y), \quad (2)$$

where Y – the grams of oleoresin extracted per 100 g of dry ginger (initially at a time, $t = 0$: $Y = 0$); K – the maximum yield of oleoresin which can be extracted in the process per 100 g of dry ginger; t – the extraction time, min; τ – the time constant for the process, min.

This model is a lumped form of Fick's law of diffusion (Halim et al., 2012). Solving the differential equation gives:

$$Y(t) = K\left[1 - e^{-\frac{t}{\tau}}\right]. \quad (3)$$

The maximum yield (K) and time constant (τ) depend on the solvent used and the ratio (R, ml of solvent used per 1 g of dry ginger used). This equation matches Patricelli et al. (1979) model without a washing stage. The resulting integration results presented in equation 3 were employed to model the extraction kinetics for the process.

Other kinetics models reported for solid-liquid extraction processes include Peleg, Power-law, Parabolic diffusion, Elovich model, Weibull, Patricelli's 2-step, as well as So and Macdonald models, that would aid the understanding of the extraction mechanism were also investigated. The models were adopted from literature (Billel et al., 2016; Hanatou et al., 2007; Chinedu and Albert, 2020; Ana-marija et al., 2018; Kasuma and Mahfud, 2017; Nour et al., 2020). Table 1 presents the mathematical expression for these models.

Table 1 – List of other kinetic models

Model	Mathematical expression	References
Peleg / 2nd-order / Hyperbolic	$Y = \frac{t}{(1/K_1) + (t/K_2)}$	Billel et al., 2016; Hanatou et al., 2007; Chinedu and Albert, 2020; Ana-marija et al., 2018; Kasuma & Mahfud, 2017.
Power law	$Y = K_3 * t^{K4}$	Billel et al., 2016; Chinedu & Albert, 2020.
Parabolic diffusion	$Y = K_5 + K_6 * t^{0.5} + +K_7 * t$	Billel et al., 2016; Chinedu and Albert, 2020.
Elovich / Logarithmic	$Y = K_8 + K_9 ln(t)$	Billel et al., 2016; Chinedu and Albert, 2020.
Weibull	$Y = 1 - e^{(-(t/K_{10})^{K_{11}})}$; $K_{11} < 1$	Billel et al., 2016.
Patricell's 2-step	$Y = K_{12(1-e^{(-t/T_1)})} + +K_{13(1-e^{(-t/T_2)})}$	Billel et al., 2016; Nour et al., 2020.
So and Macdonald	$Y = K_{14(1-e^{(-t/T_3)})} + +K_{15(1-e^{(-t/T_4)})} + +K_{16(1-e^{(-t/T_5)})}$	Billel et al., 2016.
Exponential	$Y = K_{17} \cdot e^{(T_6 \cdot t)}$	Nour et al., 2020.

Notes: Y is the yield of oil extracted at time t; t is the extraction time; K_1 is the maximal rate constant; K_2 is the corresponding highest yield; K_3 is characteristic of a carrier-active agent; K_4 is the diffusion exponent; K_5 is a hyperbolic model parameters extraction rate at the beginning (1/min); K_6 is the constant related to maximum extraction yield (1/min); K_7 is parabolic model constant; K_8 and K_9 are the constants of the logarithmic model; K_{10} is the diffusion rate parameter; K_{11} is the diffusion exponent; T_1, T_2, T_3, T_4, and T_5 are the mass transfer coefficients for the washing step, the diffusion step, the washing step, the slow diffusion step, and the very slow diffusion step, respectively; T_6 is the rate constant; K_{12}, K_{13}, K_{14}, and K_{15} are the lipid yield at equilibrium for the washing step, the diffusion step, the washing step, the slow diffusion step, and the very slow diffusion step, respectively; K_{17} is the yield at $t = 0$, in line with the references cited.

2.5 Process model development

With MATLAB, an algorithm was developed for modeling the extraction kinetics for the prediction of extraction rate in the form oleoresin yield via the use of a curve-fitting approach (to fit the theoretical model presented in equation 3) with the use of the data collected from the laboratory studies. For the curve fitting, model development, and validation, the MATLAB algorithm has been used.

The developed models' accuracy was evaluated using statistical parameters such as R-squared value, root-mean-square-error (RMSE), and the sum of square error (SSE). The graphical representation of the effect of time and particle size on the extraction process was done using a Python library known as 'matplotlib,' the algorithm

employed for the representation. Results were collected for the different sets of experimental data for the different particle sizes.

Furthermore, the selected first-order kinetics model's accuracy was further revised to improve its accuracy by introducing regression terms such as constant, linear, and nonlinear terms that were investigated to develop an improved first-order kinetic model with the aid of programmed code.

3 Results and Discussions

3.1 Preliminary analysis of the ginger rhizomes

The sample was identified at Biological Science Department ABU Zaria. The ginger was identified as zingeber officinale. Based on the results collected and presented in our previous studies (Ameh et al., 2020) for the proximate analysis of dry ginger rhizomes, it was identified that the proximate composition of the ginger rhizome compares favorably with those in literature. Slight variations observed could be attributed to the season, climate, storage condition, and ginger species. Furthermore, the ginger was reported to have displayed a moisture content of 6.4 %, which is lower than that obtained by El-Ghorab et al. (2010) but similar to that obtained by Otunola et al. (2010). The dry ginger sample's major component was the crude carbohydrate content with a high total carbohydrate value of 59.8 % and the crude fiber content of 9.7 %. The protein content is important from the nutritional point of view. This protein content was obtained as 9.8 % from the dried ginger sample analyzed.

Also, the review of the literature reveals that the works of Mbaeyi-Nwaoha et al. (2013) and Otunola et al. (2010) showed a relatively low protein content compared to this value, while Latona et al. (2012) reported a higher value. It should be noted that the low moisture content of the ginger samples significantly raises the other constituents. The dry ginger sample's crude fat content was 8.8 %, whereas the ash content is 5.5 %, which is comparable to values obtained in literature, where the total ash content of dry ginger has been reported to be 6.1 % (El-Ghorab et al., 2010).

The FTIR analysis presented in the previous studies (Alewo et al., 2020) indicated that the ginger oleoresin has hydroxyl, carbonyl, alkane, alkyl, and ketones functional groups present in its spectra. Other compounds that were confirmed present include phenolic compounds, which were similar to what was obtained in the literature (Purnomo et al., 2010; Jayanudin et al., 2015; 2017).

3.2 Effect of particle size and extraction time on oleoresin yield

The effect of particle size and extraction time, t, on solid-liquid extraction of oleoresin with ethyl acetate at 40 °C, and the solid-liquid ratio of 10 g/100 ml solvent was evaluated with the aid of the statistical plot represented in Figure 1, which shows the relationship between various variables.

Furthermore, the high initial rate of oleoresin extraction obtained within in the first 10 minutes was found to be 5.1 % at 1200 µm and 7.5 % at 250 µm for the least and highest initial rate, respectively, which can be seen from the extraction curves, followed by slower extraction rate which asymptotically approaches the equilibrium concentration. These findings indicate that smaller particle size promotes the oleoresin extraction process rate while larger sizes retards the extraction process rate and reduce that quantity obtainable within a limited extraction time.

The extraction curves of Figure 1 exhibited an exponential pattern for all particle sizes considered. The extracted oleoresin yield was inversely proportional to particle size, with the highest yield (9.3 %) recorded with 250 µm and the least (5.1 %) recorded with 1200 µm. Relating the results obtained for ethyl acetate's use indicated that it was lower than the use of ethanol reported by Ameh et al. (2020) as 10.4 % as its highest yield obtainable.

The lowest initial yield reported for the use of ethanol (5.8 %) was found to be greater than that recorded for the use of ethyl acetate (5.1 %) at the same 10 minutes extraction time in Alewo et al. (2020) report. The relative drops in the trend line or extraction rate compared to ethanol in the report of Ameh et al. (2020) indicate that ethyl acetate's choice to ethanol is not good enough.

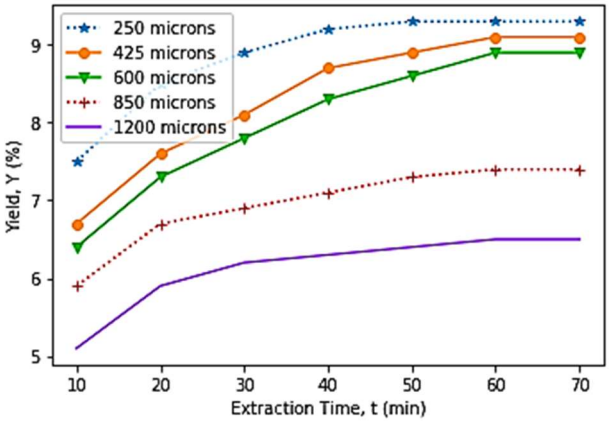

Figure 1 – Particle size effect on oleoresin extraction from ginger with ethyl acetate at 40 °C and L/S Ratio = 10 g/100 ml for different extraction time.

Moreover, ethyl acetate, which yields 9.3 %, was found not to be better than ethanol, which yields 10.4 % at the same condition (70 min, 40ºC, 250 microns, and L/S Ratio = 10 g/100 ml). The highest yield (9.3 %) obtained was lower than reported by Nguyen et al. (2018) as 9.7 % using ethanol at a larger particle size of 2mm or 2000 µm. However, this study's highest yield was found to be higher than 8.15 %, which was reported by Saidi et al. (2014) as its highest oleoresin yield at 35 °C temperature and 25 MPa pressure using ultrasound-assisted supercritical carbon dioxide extraction approach.

This behavior could be attributed to the large surface area possessed by the smaller particle-sized ginger powder, which resulted in high yield within the first 10

minutes. After that, the rate slowed down, as shown in Figure 2.

Also, the results obtained for this study were much lower than the Nguyen et al. (2018) report, which employed microwave energy and a different solvent (known as ethanol). While Saidi et al. (2014) yield were found to be lower than the results obtained for the highest yield in this study, which traced to be dues to the lower temperature used in Saidi et al. (2014) studies using same particle size (250 microns). This deduction demonstrates the significance of the temperatures in an extraction process.

3.3 The 1st order kinetics models developed

The results of the model developed, its parameters (or coefficients), R-squared value, and the root-mean-square-errors (RMSE) from the model validation analysis carried-out are presented in Table 2 with 95 % confidence bounds.

Table 2 – Model developed parameters

Size, μm	*K*	*T*, min
1200	6.377	6.510
850	7.211	6.188
600	8.545	8.336
425	8.805	7.952
250	9.182	6.201

In Table 2, the use of 250 μm particle size displayed 9.2 % as the maximum grams of oleoresin which can be extracted in the process per 100 g dry ginger, *K*, while the 1200 μm shows that lowest maximum yield (*K*) as 6.4 % despite showing a close time (*T*) constant of 6.201 and 6.5 minutes for 250 μm and 1200 μm, respectively. The comparison of the highest yield's *K* and *T* for 250 μm, it was deduced that the *K* recorded for the use of ethyl acetate in this study is lower than when ethanol (10.3 %) is used. Also, the literature survey indicated that the time constant (*T*) for the use of ethyl acetate (in this study) was much longer than the case of using ethanol, which was reported as $T = 4.03$ minutes by Alewo et al. (2020) at the same confidence level of 95 % bound.

From the results presented in Table 2, it can be deduced that the K (the maximum grams of oleoresin which can be extracted in the process per 100 g of dry ginger) decreases as the particle size of the ginger increases, which agrees with the curve presented on Figure 2 (showing the effect of particle size on yield). It was found that 250 μm recorded the highest maximum extractable oleoresin from 100 g of dry ginger as 10.3 g, while 1200 μm recorded the least as 8.5 g oleoresin per 100 g of dry ginger.

It was also deduced from Table 2 that the higher the ginger's particle size, the larger the time constant (*T*) becomes. As the particle size rises from 250, 425, 600, and 850 μm to 1200 μm, their time constant values become larger from 4.03, 6.32, 7.03, and 9.85 min 10.22 min, respectively. It was deduced that the 1200 μm model recorded the highest time constant while 250 μm models recorded the least.

3.4 Development of an improved 1st order model and analysis of other selected models

Figure 2 graphically presents the model of the agreement that existed between the experimental and model-predicted values.

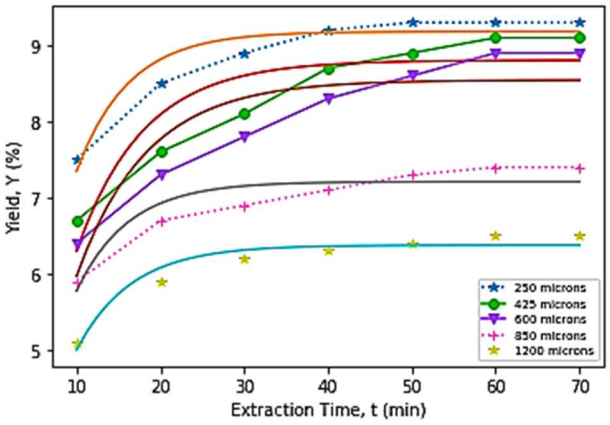

Figure 2 – 1st-order model for the extraction

Figures 3–5 present the effect of introducing a regression function (linear/nonlinear) or constant in the first-order model. In contrast, the use of a second-order model and Patricell's 2-step models were also presented in Figures 8 and 9.

The results presented in Figure 2 indicated that the unmodified 1st-order model displayed a poor agreement for the oleoresin extraction from ginger with all the particle size, especially at the lower extraction times compared to the high extraction time which shows a better relation with experiment. In general, it was not good enough.

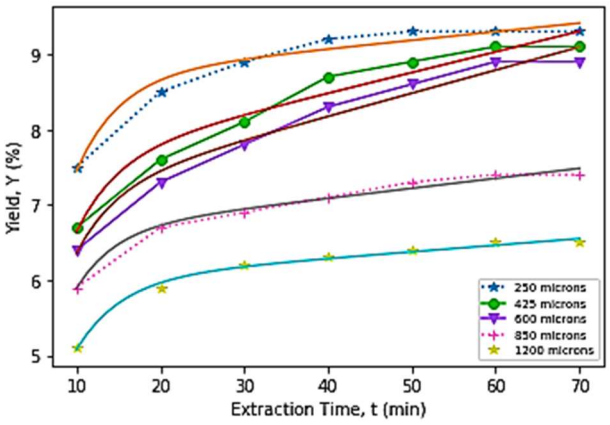

Figure 3 – Model improved with nonlinear (t/K_2) in the 1st-order model

As a way of improving the accuracy of the 1st order model, the introduction of linear terms, $K_2 \cdot t$ and t/K_2 were investigated, and the results obtained presented in Figure 3 (for t/K_2), which reflect that the introduction of t/K_2 yielded poorer predictions while the no optimal solution was obtained for the use of $K_2 \cdot t$.

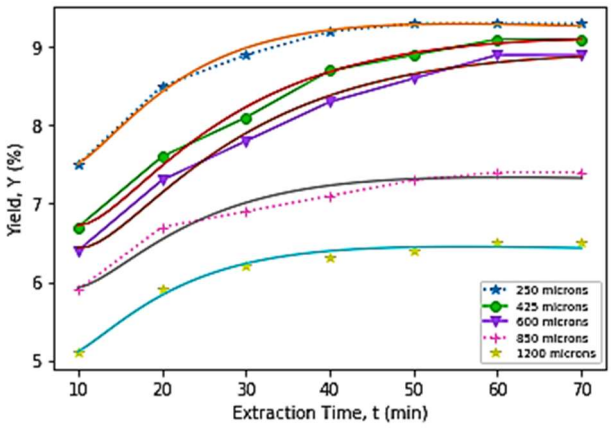

Figure 4 – Model improved with the introduction of nonlinear (K_2/t) in the 1st-order model

The assessment made for the use of the nonlinear function, K_2/t shown in Figure 4 reveals a good agreement with the experimental values suggesting that the introduction of nonlinear regression terms would best improve the model prediction accuracy the use of linear terms assessed. The revised form of the first-order model (presented in equation (3)) with the introduction of the non-linear term is expressed as:

$$Y(t) = K_1\left[1 - e^{-\frac{t}{\tau}}\right] + \frac{K_2}{t}. \qquad (4)$$

Further investigation of the constant (K_2) introduction was investigated, whose results are presented in Figure 5. The profile indicated that the constant introduction significantly improved the model's prediction, displaying a good fitting with experiment across different particle sizes studied.

The first-order model presented in equation (3) improved with the introduction of constant term graphically presented in Figure 5 is expressed as:

$$Y(t) = K_1\left[1 - e^{-\frac{t}{\tau}}\right] + K_2. \qquad (4)$$

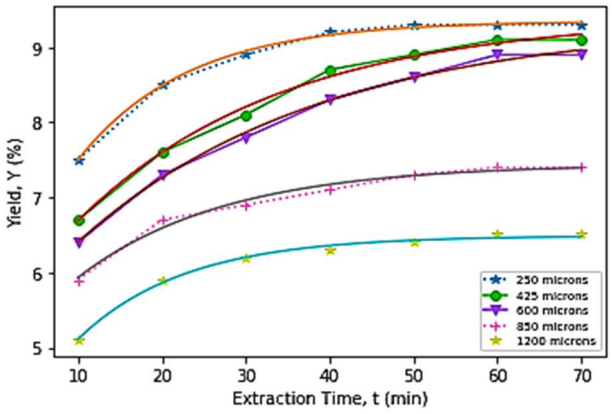

Figure 5 – Model improved with the introduction of constants in the 1st-order model

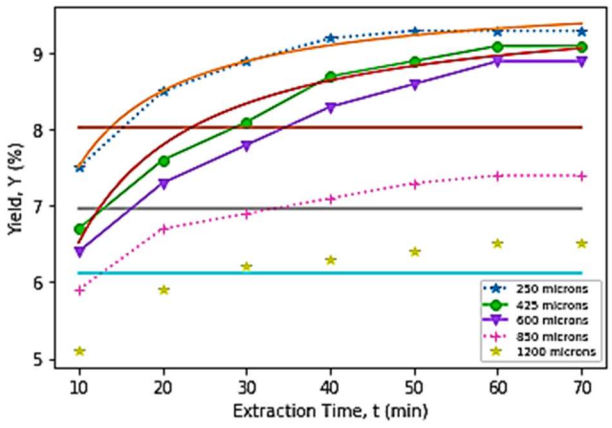

Figure 6 – 2nd-order model for extraction

Alternative assessment of 2nd order and Patricelli's 2-step models presented in Figures 6 and 7 reveal that the second-order model (in Table 1) shows poor relation with the experimental value, especially for higher particle sizes signifying poor fitness with experimental values. In comparison, Patricelli's 2-step model (in Table 1) shows a better relationship with the experiment indicating the reaction mechanism potentially two steps, following the report of literature (Billel et al., 2016; Nour et al., 2020).

In general, the introduction of either constant term or nonlinear regression terms in a first-order model effectively improves its prediction. However, the use of Patricelli's 2-step models was found to have proven to be good potential.

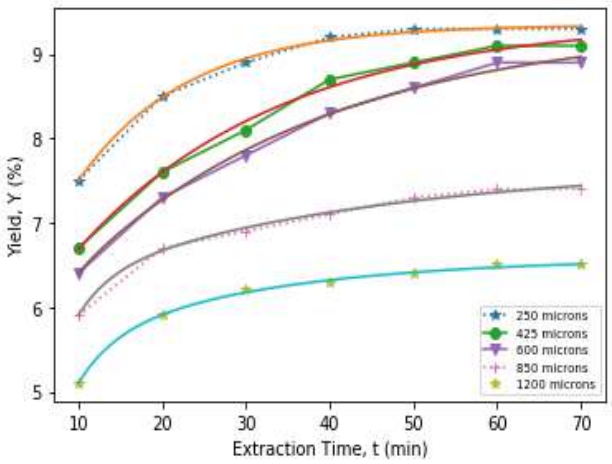

Figure 7 – Patricelli's 2-step model for extraction

3.5 Statistical analysis of the developed models

The statistical analysis of the unmodified first-order models, improved ones, and other selected models investigated are presented in Table 3, displaying the accuracy in term R-squared values obtained across the different sizes considered in this study. In accordance with the results presented for the average R-square values for the use of different models presented in Table 3, the accuracy (in term of average R-squared value)

was found to be in the order of FO (87.5 %) < FO+NL (98.5 %) < FO+C (99.4 %) < PTS (99.7 %).

Table 3 – R-square value for the different models

PS, μm	FO	FO + C	FO + NL	PTS
1200	0.9397	0.9947	0.9838	0.9985
850	0.8715	0.9860	0.9622	0.9953
600	0.8138	0.9966	0.9891	0.9966
425	0.8269	0.9944	0.9927	0.9944
250	0.9215	0.9976	0.9946	0.9976
Average	0.8747	0.9939	0.9845	0.9965

Note: FO is the 1st-order model, FO + C is the first-order model with the introduction of the constant term, FO + NL is the first-order model with the introduction of the nonlinear term, TS is the Patricelli's two-steps model, and PS is the particle size in microns.

Based on the results collected for the average R-squared values in Table 3, it can be said that the introduction of either constant term and nonlinear term in the first-order model significantly improved the kinetic model prediction displaying a good fit with the experimental data like the use of Patricelli's two-steps model. This finding suggests that the solid-liquid extraction process potentially involved two steps (that is, washing and diffusion steps) in line with the literature report (Billel et al., 2016; Nour et al.,2020).

Table 4 – The coefficient of the FO + C

PS, μm	K_1	*T*, min	K_2
1200	3.02	12.71	3.46
850	2.68	17.46	4.76
600	4.14	28.96	5.20
425	4.09	24.46	5.31
250	3.97	13.07	5.37

The results presented in Tables 4 and 5 show that the model coefficients obtained using the improved first-order model (with the introduction of a constant term, K_2), and Patricelli's 2-step model. The parameters or coefficients presented an improved model (FO+C) for the oleoresin extraction in Table 4 could imply that K_1 (that is, the rate constant reciprocal or mass transfer coefficient) and T indicated the kinetics for step 1 (washing step). In contrast, K_2 (that is, mass transfer coefficient or reciprocal of the rate constant) could account the step 2 (diffusion step) following literature (Nour et al., 2020) when compared to Patricelli's step, which indicated a good correlation with the experiment.

However, the extraction kinetics is strongly dependent on the diffusion step due to the consistent higher K_2 compared to K1. This diffusion coefficient is largely dependent on the particle size. In contrast, extraction time shows lesser effect than the particle size effect in line with Billel et al. (2016) and Nour et al. (2020) for 2-step extraction kinetics.

The result shown in Table 5 equally accounts for the contribution of two-step mechanism K_1 and K_2, with the inclusion of time dependency where T_1 and T_2 depict the kinetics involved in each step, washing and diffusion step, respectively.

Table 5 – The coefficient of the PST

PS, μm	K_1	T_1, min	K_2	T_2, min
1200	5.13	4.43	1.46	23.34
850	5.99	4.01	1.69	36.07
600	5.29	2.09	4.07	30.02
425	5.31	0.05	4.09	24.46
250	3.97	13.07	5.37	0.39

From which it deduced that for extraction carried out for higher particle sizes (PS = 1200 μm) first step was rapid (T_1 = 4.43 min) and higher equilibrium yield (K_1 = 5.13) but encountered higher diffusion resistance resulting in lower equilibrium yield (K_2 = 1.46) at diffusion step with poor diffusion rate (T_2 = 23.34 min). This deduction was found to be similar for size except for 425 and 250 μm that were different, where the extraction that was held at 425 microns was found to be rapid (T_1 = 0.05 min, K_1 = 5.31) at the first step and stronger mass transfer resistance make the diffusion rate to be slow (T_2 = 24.46 min, K_2 = 4.09).

Unlike 250 μm, which encountered stronger resistance (T_1 = 13.07 min, K_1 = 3.97) at the first step but displayed a lesser resistance for the diffusion step (T_2 = 0.39 min, K_2 = 5.37). This stronger resistance experienced in the first step for the use of 250 μm could be improved by using a rise in temperature employed in the extraction process. This inference was found to be in line with the report of Hanatou et al. (2007) and Ana-Marija et al. (2018) that indicated that temperature rise would help overcome extraction resistance.

4 Conclusions

The insight into the significance of ethyl acetate in the extraction of oleoresin from ginger rhizome via the investigation of the influence of particle size and extraction time on the oleoresin yield was studied. The extraction kinetics was also successfully modeled for the yield of oleoresin via the use of a curve-fitting approach aided with the use of tools like MATLAB and Python algorithm.

Findings from this study reveal that the choice of using ethyl acetate to the use of other solvents such as ethanol is not good enough comparatively in terms of yield.

Moreover, for each ginger particle size considered, the yield of oleoresin increases with increasing extraction time up to an optimum time, after which the yield remains constant. The optimum extraction was found to increase with decreasing particle size. Thus, the Patricelli parameter T was found to be a particle size-dependent parameter. Also, the maximum oleoresin yield was found to be dependent on particle size: smaller particle sizes favored high yield, and the Patricelli parameter K was found to be particle size-dependent, where 250 μm show the high yield with 9.3 %.

The kinetics studies reveal that using a single step first-order model (Patricelli's first-order kinetic model) shows 87 % fitness with the experimental data. With the introduction of the constant term accounting for the

diffusion step separately (as an addition), the model's fitness was found to have risen to 99 % with the experimental data. The improved form of Patricelli's first-order kinetic model was found to have shown as good agreement with the prediction of Patricelli's 2-step kinetic model. The study also confirms that the oleoresin extraction process in the presence of ethyl acetate was found to be first-order kinetics involving two steps mechanism where the use of a single-step first-order model (Patricelli's first-order kinetic model). And the choice of using ethyl acetate must have contributed to the strong resistance present in the first step of the extraction mechanism, especially for the smaller particle size (250 μm) due to the high time constant, T_1 = 13 min (that is, the lower rate constant) for its 2-step mechanism models.

Therefore, it is recommended that further studies look into the use of alternatives solvents, and the effect of higher temperatures on this extraction process can also be investigated.

References

1. Akhihiero, E. T., Ayodele, B. V., Akpojotor, G. E. (2013). Effect of particle size and temperature variation on the yield of essential oil from lemongrass using steam distillation. *African Journal of Physics,* Vol. 6, pp. 105–112.
2. Ameh, A. O., Olakunle, M. S., Shehu, H. U., Oyegoke, T. (2020). Kinetics of the extraction of oleoresin from ginger: Influence of particle size and extraction time effects. *NIPES Journal of Science and Technology Research*, Vol. 2(2), pp. 142–151.
3. Azian, N. M., Sazalina, M. S., Rizan, H. M. R. (2001). *Essential Oil and Active Ingredients Extraction from Ginger Plants*, Annual Progress Report Centre of Lipids Engineering and Applied Research, Kuala Lumpur, Malaysia.
4. Bartley, J. P., Jacobs, A. L. (2000). Effects of drying on flavor compounds in Australian-grown ginger (Zingiber officinale). *Journal of the Science of Food and Agriculture,* Vol. 80(2), pp. 209–215.
5. Bode, A. M., Dong, Z., (2011). *The Amazing and Mighty Ginger.* In: Benzie IFF, Wachtel-Galor S, editors. Herbal Medicine: Biomolecular and Clinical Aspects. 2nd edition. Boca Raton (FL): CRC Press/Taylor and Francis.
6. Carenas, E, Packer, L, (1996). *Handbook of Antioxidants*. Plenum, New York. pp. 127–131.
7. El-Ghorab, A. H., Nauman, M., Anjum, F. M., Hussain, S., Nadeem, M. (2010). A comparative study on chemical composition and antioxidant activity of ginger (Zingiber officinale) and Cumin (Cuminum cyminum). *J. Agric. Food Chem.*, Vol. 58, pp. 8231–8237.
8. Halim, R., Danquah, M. K., Webley, P. A. (2012). Extraction of oil from microalgae for biodiesel production: A review. *Biotechnology Advances,* Vol. 30, pp. 709–732.
9. Hassan, H. A., et al. (2012). Chemical composition and antimicrobial activity of the crude extracts isolated from zingiber officinale by different solvents. *Pharmaceut Anal Acta,* Vol. 3, pp. 184.
10. Hemwimon, S., Pavasant, P., Shotipruk, A. (2007). Microwave-assisted extraction of antioxidative anthraquinones from roots of Morinda citrifolia. *Separation and Purification Technology*, Vol. 54 (1), pp. 44–50.
11. Ismail, R. K., Devender, K., Lingam, A., Jagan, M. R. (2013). Effect of microwave-assisted extraction on the release of polyphenols from ginger (Zingiber officinale). *International Journal of Food Science and Technology*, Vol. 48, pp. 1828–1833.
12. Jakopic, J., et al. (2009). Extraction of phenolic compounds from green walnut fruits in different solvents. *Acta Agriculturae Slovenica*, Vol. 93 (1), pp. 11–15.
13. Jayanudin, J., Rochmadi, R., Renaldia, M. K., Pangihutana, P. (2017). The influence of coating material on encapsulation efficiency of red ginger oleoresin. *ALCHEMY Jurnal Penelitian Kimia*, Vol. 13(2), pp. 275–287.
14. Jayanudin, J., Rochmadi, R., Wiratni, Y., Yulvianti, M., Barleany, D. R., Ernayati, W. (2015). Encapsulation of red ginger oleoresin (Zingiber officinale var. rubrum) with chitosan - alginate as wall material using spray drying. *Research Journal of Applied Sciences, Engineering and Technology*, Vol. 10, pp. 1370–1378.
15. Kanadea, R., Bhatkhandeb, D. S. (2016). Extraction of ginger oil using different methods and the effect of solvents, time, temperature to maximize yield. *International Journal of Advances in Science Engineering and Technology*, Vol. 4(3), pp. 241–244.
16. Kim, E., Min, J., Kim, T., Lee, S., Yang, H., Han, S., Kim, Y., Kwon, Y., (2005). [6]-Gingerol, a pungent ingredient of ginger, inhibits angiogenesis in vitro and in vivo. *Biochemical and Biophysical Research Communications*, Vol. 335(2), pp. 300–308.
17. Kim, J. H., Shin, H. K., Seo, C. S. (2014). Optimization of the extraction process for the seven bioactive compounds in Yukmijihwang-tang, an herbal formula, using response surface methodology, *Pharmacogn Mag.,* Vol. 10(3), pp. S606–S613.
18. Latona, D. F., Oyeleke, G. O., Olayiwola, O. A. (2012). Chemical analysis of ginger root. *IOSR Journal of Applied Chemistry*, Vol. 1(1), pp. 47–49.
19. Mbaeyi-Nwaoha, I. E., Okafor, G. I., Apochi, O. V., (2013). Production of oleoresin from ginger (Zingiber officinale) peels and evaluation of its antimicrobial and antioxidative properties. *African Journal of Microbiology Research*, Vol. 7(42), pp. 4981–4989.
20. Mukherjee, S., Mandal, N., Dey, A., Mondal, B. (2014). An approach towards optimization of the extraction of polyphenolic antioxidants from ginger (Zingiber officinale). *Journal of Food Science and Technology*, Vol. 51(11), pp. 3301–3308.
21. Dung, N. T., Duc, T. H., Dang, N., Thanh, B. (2018). Optimization of ginger oleoresin extraction from fresh ginger by using microwave-assisted energy. *Vietnam Journal of Science and Technology*, Vol. 56(4A), pp. 229–237.
22. Ok, S., Jeong, W. (2012). Optimization of extraction conditions for the 6-Shogaol-rich extract from ginger (Zingiber officinale Roscoe). *Prev Nutr Food Sci.*, Vol. 17, pp. 166–171.

23. Otunola, G. A., Oloyede, O. B., Oladiji, A. T., Afolayan, A. J. (2010). Comparative analysis of the chemical composition of three spices – Allium sativum L., Zingiber officinale Rosc. And Capsicum frutescens L. commonly consumed in Nigeria. *African Journal of Biotechnology*, Vol. 9(41), pp. 6927–6931.
24. Ozkal, S. G., Yener, M. E., Bayindirli, L. (2005). Response surfaces of apricot kernel oil yield in supercritical carbon dioxide. LWT-Food Science and Technology, Vol. 38, pp. 611–615.
25. Patricelli, A., Assogna, A., Casalaina, A., Emmi, E., Sodini, G. (1979). Fattori che influenzano l'estrazoine dei lipidi da semi decorticate di girasole. *La Rivista Italiana Delle Sostanze Grasse*, Vol. 56, pp. 136–142.
26. Platel, K., Srinivasan, K. (1996). Influence of dietary spices or their active principles on digestive enzymes of small intestinal mucosa in rats. *International Journal of Food Sciences and Nutrition,* Vol. 47, pp. 55–59.
27. Purnomo, H., Jaya, F., Widjanarko, S. B. (2010). The effects of type and time of thermal processing on ginger (Zingiber officinale Roscoe) rhizome antioxidant compounds and its quality. *International Food Research Journal,* Vol. 17, pp. 335–347.
28. Saidi, P. P., Arya, O. P., Pradhan, R. C., Singh, R. S., Rai, B. N., (2014). Separation of oleoresin from ginger rhizome powder using green processing technologies. *Journal of Food Process Engineering*, Vol. 38(2), pp. 1745–4530.
29. Salmon, C. N. A., et al. (2012). Characterization of cultivars of Jamaican ginger (Zingiber officinale Roscoe) by HPTLC and HPLC. *Food Chemistry,* Vol. 131, pp. 1517–1522.
30. Stoilova, I., Krastanov, A., Stoyanova, A., Denev, P, Gargova, S. (2007). Antioxidant activity of a ginger extract (Zingiber officinale). *Food Chemistry*, Vol. 102(3), pp. 764–770.
31. Yang, Y., et al. (1995). Combined temperature & modifier effects on supercritical CO_2 extraction efficiencies of polycyclic aromatic hydrocarbons from environmental samples. *Analytical Chemistry*, Vol. 67(3), pp. 641–646.
32. Zhiyi, L. Xuewu, L. Shuhua, C. Xiaodong, Z. Yuanjing, X. Yong, W., Feng, X. (2006). An experimental and simulating study of supercritical CO_2 extraction for pepper oil. *Chemical Engineering and Processing: Process Intensification*, Vol. 45(4), pp. 264-267.
33. Hadrich, B., Dimitrov, K., Kriaa, K. (2017). Modeling investigation and parameter study of polyphenols extraction from carob (Ceratonia siliqua L.) using experimental factorial design. *Journal of Food Processing and Preservation*, Vol. 41(2), e12769.
34. Harouna-Oumarou, H. A., Fauduet, H., Porte, C., and Ho, Y. S. (2007). Comparison of kinetic models for the aqueous solid-liquid extraction of Tilia sapwood in a continuous stirred tank reactor. *Chemical Engineering Communications*, Vol. 194(4), pp. 537–552.
35. Agu, C. M., Agulanna, A. C. (2020). *Kinetics and Thermodynamics of Oil Extracted from Amaranth. Nutritional Value of Amaranth*. IntechOpen.
36. Cvetkovic, A. et al. (2018). The estimation of kinetic parameters of the solid-liquid extraction process of the lavender flower (Lavandula x hybrida L.). *Croatian Journal of Food Science and Technology*, Vol. 10(1), pp. 64–72.
37. Kusuma, H. S., Mahfud, M. (2017). Comparison of kinetic models of oil extraction from sandalwood by microwave-assisted hydrodistillation. *International Food Research Journal*, Vol. *24*(4), pp. 1697–1702.
38. Zghaibi, N., Omar, R., Kamal, S. M. M., Biak, D. R. A., Harun, R. (2020). Kinetics study of microwave-assisted brine extraction of lipid from the Microalgae Nannochloropsis sp. *Molecules*, Vol. 25(4), pp. 784.
39. Lin, C. B., Jingwen, P., Ali, A. (2018). Extraction kinetics of Ziziphus jujuba fruit using solid-liquid extraction. *Journal of Engineering Science and Technology*, Vol. 13, pp. 27–39.